



## CHANGES IN NUCLEAR CHROMATIN PRECEDE INTERNUCLEOSOMAL DNA CLEAVAGE IN THE INDUCTION OF APOPTOSIS BY ETOPOSIDE

XIAO-MING SUN, ROGER T. SNOWDEN, DAVID DINSDALE, MICHAEL G. ORMEROD and  
 GERALD M. COHEN\*

MRC Toxicology Unit, Centre for Mechanisms of Human Toxicity, Hodgkin Building,  
 University of Leicester, P.O. Box 138, Lancaster Road, Leicester LE1 9HN, U.K.

(Received 12 July 1993; accepted 11 October 1993)

**Abstract**—Etoposide, a DNA topoisomerase II inhibitor, caused a concentration-dependent induction of apoptosis in immature thymocytes. Using a flow cytometric method to separate and quantify normal and apoptotic cells, etoposide-induced apoptosis was inhibited by cycloheximide and actinomycin D but not by zinc. Etoposide induced a marked cleavage of DNA into nucleosomal length fragments or multiples thereof, which was completely inhibited if the thymocytes were also incubated in the presence of zinc. Etoposide, alone, induced the classical ultrastructural features of apoptosis, but in the presence of zinc, the morphological pattern was markedly different and dominated by discrete clumps of condensed chromatin abutting the nuclear membrane. These latter changes resemble those described as the earliest changes in apoptosis. These results support the hypothesis that, in the induction of apoptosis, critical alterations in nuclear chromatin occur prior to endonuclease cleavage of DNA into nucleosomal fragments.

Apoptosis is a form of active cellular self destruction or cell suicide [1–3]. It is a major form of cell death occurring in a wide variety of different biological systems and is characterized by chromatin condensation and a requirement for energy as well as RNA and protein synthesis [2–4]. Biochemically, apoptosis has been best characterized by the cleavage of DNA into nucleosomal size fragments of 180–200 bp, or multiples thereof, which are detected by gel electrophoresis as a DNA ladder [5, 6]. A number of agents including glucocorticoids,  $\gamma$ -irradiation, the calcium ionophore A23187, tributyltin oxide, and anti-CD3 antibodies, induce apoptosis in immature thymocytes [2, 3, 7, 8]. Recently, it has been observed that a number of anticancer agents may exert their action, at least in part, by increasing apoptosis and a better understanding of these mechanisms may lead to the development of novel anticancer agents [9, 10].

DNA topoisomerases are important nuclear enzymes, whose function is to resolve topological problems in DNA [11]. Two major topoisomerases, types I and II, have been found in all eukaryotic cells, which function by forming transient enzyme-bridged DNA breaks on one (type I) or both DNA strands (type II) [11, 12]. DNA topoisomerase II is an important intracellular target for a number of clinically useful antitumour drugs, including the epipodophyllotoxin, etoposide (VP-16). These drugs interfere with the breakage-rejoining reaction of topoisomerase II, by trapping a covalently linked complex of the enzyme and the 5' cleaved termini of the DNA molecule, known as a cleavable complex [11, 13]. The cleavable complexes appear responsible

at least in part for a number of cellular effects of topoisomerase poisons, including cell death and elevated levels of sister chromatid exchange and chromosome aberrations [11]. In general, there is a good relationship between cleavable complex formation and cytotoxicity, although exceptions have been observed suggesting the importance of other cellular processes [14]. Results using a human colonic carcinoma cell line suggest that in addition to topoisomerase II-mediated DNA breaks, calcium-dependent cellular processes are required for cell killing [15]. The mechanism by which the lesions induced by topoisomerase inhibitors induce cell death is unclear [14–17].

Cycloheximide, an inhibitor of protein synthesis, prevents the cytotoxicity of etoposide without altering the extent of the DNA lesions [18]. This data, together with a number of other studies suggest that DNA topoisomerase II inhibitors induce apoptosis in some cells including thymocytes [19], initially by an interaction with topoisomerase II, followed by an endonuclease cleavage of DNA [19]. Recently, we have shown that whilst zinc prevented dexamethasone-induced DNA fragmentation and internucleosomal cleavage, it did not prevent key early morphological changes of apoptosis [20]. In this study, we demonstrate that etoposide induces all the characteristic morphological and biochemical changes of apoptosis in thymocytes. Zinc, an inhibitor of the endonuclease, prevents some but not all of these changes.

### MATERIALS AND METHODS

**Materials.** Etoposide (VP-16), dexamethasone, actinomycin D, cycloheximide, Hoechst 33342, propidium iodide and Percoll were obtained from

\* Corresponding author. Tel. (0533) 525589; FAX (0533) 525616.

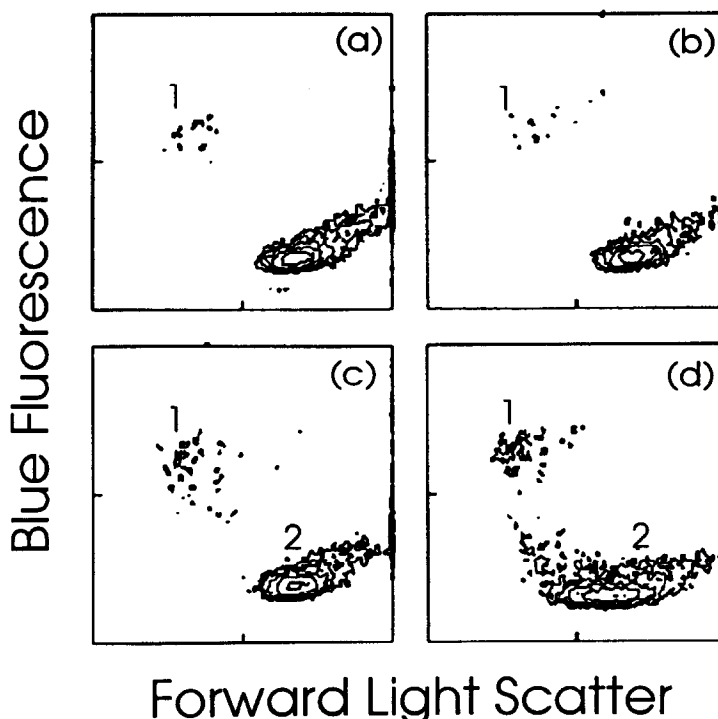


Fig. 1. Flow cytometric determination of the induction of apoptosis in thymocytes by etoposide. Thymocytes ( $2 \times 10^7$  cells/mL) were incubated for 4 hr either alone (a) or in the presence of 1 (b) and 10 (c)  $\mu$ M etoposide, or with etoposide (10  $\mu$ M) in the presence of zinc (1 mM) (d). The cells were then spun down and resuspended in medium together with Hoechst 33342 for 10 min as described in Materials and Methods. Propidium iodide was added and the cells examined by flow cytometry. Non-viable cells were gated out and two populations of viable cells separated, i.e. normal cells in region 2 with low blue fluorescence and higher forward light scatter and apoptotic cells in region 1 with high blue fluorescence and lower forward light scatter.

the Sigma Chemical Co. (Poole, U.K.). Zinc diacetate was from Fisons Scientific (Loughborough, U.K.). Density marker beads were from Pharmacia LKB, Biotechnology AB (Uppsala, Sweden).

**Thymocyte incubations.** Isolated rat thymocytes were prepared from male Fischer 344 rats (4–5 weeks old) as described previously [8] and the resulting cell suspension was diluted with RPMI 1640 containing 10% foetal bovine serum to give a final cell suspension of  $18\text{--}20 \times 10^6$  cells/mL. Incubations were carried out for up to 4 hr at  $37^\circ$  under an atmosphere of 95% air:5%  $\text{CO}_2$  with dexamethasone (0.1  $\mu$ M), etoposide (1–25  $\mu$ M), cycloheximide (10  $\mu$ M), actinomycin D (1  $\mu$ M) or zinc diacetate (1 mM).

**Flow cytometry.** A flow cytometric method was used to separate and quantify normal and apoptotic thymocytes [21]. Cells ( $2 \times 10^6$ ) were incubated with Hoechst 33342 (1  $\mu$ g/mL) for 10 min at  $37^\circ$ , cooled to  $4^\circ$ , centrifuged at 400 g for 5 min and resuspended in PBS containing propidium iodide (5  $\mu$ g/mL). Flow cytometric analysis was carried out at a flow rate of 200 cells/sec using an Ortho System 50H Cytofluorograph linked to a 2150 computer system, with krypton laser excitation at 352 nm. Forward light scatter and blue (400–500 nm) versus red ( $>630$  nm) fluorescence were recorded using linear amplification. Blue fluorescent cells were gated and

displayed as a two-dimensional cytogram of blue fluorescence intensity versus forward light scatter.

**Percoll gradients.** Purified populations of normal and apoptotic thymocytes were prepared by discontinuous Percoll gradients as described previously [22]. Beads of buoyant density of 1.063, 1.075, 1.099 and 1.119 g/mL banded at the 0–60%, 60–70%, 70–80% and 80–100% Percoll interfaces, respectively (fractions F1–F4, respectively).

**Agarose gel electrophoresis and DNA fragmentation.** Agarose gel electrophoresis was used to detect DNA laddering in whole cells ( $2 \times 10^6$  cells) by the method of Sorenson *et al.* [23]. DNA fragmentation was measured by the percentage of diphenylamine-reactive material present in the 13,000 g supernatant fractions of lysed cells [24].

**Electron microscopy.** Aliquots of cell suspension (approx.  $1 \times 10^6$  cells, 0.1 mL) were fixed in 0.4 mL of 2% glutaraldehyde at room temperature for at least 30 min and then spun down. Pellets were resuspended in 0.5 mL of 2% glutaraldehyde and spun down. Resulting pellets were postfixed in 1% osmium tetroxide and stained, en bloc, in 2% aqueous uranyl acetate before being dehydrated through a series of ethanols and embedded in Araldite. Semi-thin (1  $\mu$ m) sections were cut, axially, through all layers of each pellet to select areas for

Table 1. Induction of apoptotic cells and DNA fragmentation by etoposide

Compound	Concentration ( $\mu\text{M}$ )	Viability (%)	Apoptosis (%)	DNA fragmentation (%)
Control	—	$86.3 \pm 1.9$	$8.3 \pm 1.2$	$6.6 \pm 0.9$
Etoposide	1	$81.3 \pm 2.0$	$12.3 \pm 0.9$	$16 \pm 1.7$
	5	$79.3 \pm 1.5$	$24.3 \pm 1.6$	$29.3 \pm 5.7$
	10	$79.9 \pm 2.6$	$26.8 \pm 3.4$	$33.8 \pm 4.7$
	25	$74.3 \pm 0.8$	$40.8 \pm 3.4$	$47.7 \pm 5.9$
Dexamethasone	0.1	$78.9 \pm 1.2$	$27.1 \pm 1.0$	$20.3 \pm 2.0$

Thymocytes were incubated for 4 hr either alone or in the presence of etoposide (1–25  $\mu\text{M}$ ) or dexamethasone. After incubation, either the % DNA fragmentation was determined by the diphenylamine method as described in Materials and Methods or the cells were incubated with Hoechst 33342. The % viability was assessed as the % of cells excluding propidium iodide. The % of apoptotic cells was determined by the number of cells with high blue fluorescence expressed as a % of the total number of viable cells. The results represent the mean  $\pm$  SEM of at least three separate experiments.

ultra-microtomy. Ultrathin sections were stained with lead citrate and examined in a Jeol 100-CX electron microscope.

## RESULTS

### Induction of apoptosis

Viable normal and apoptotic thymocytes were separated by flow cytometry following incubation of the cells with the vital bisbenzimidazole dye, Hoechst 33342 [21]. The non-viable cells, which included propidium iodide and fluoresced red, were gated out during the computer analysis. Two populations of viable cells were clearly distinguished: (a) normal cells in region 2 (Fig. 1a–d), which had a higher forward light scatter (indicative of a larger size) and exhibited low blue fluorescence due to the Hoechst 33342 and (b) apoptotic cells in region 1 (Fig. 1), which had a lower forward light scatter and exhibited high blue fluorescence. These cells have been shown to be apoptotic based on a number of criteria including ultrastructure and the appearance of DNA ladders on agarose gel electrophoresis [21]. Etoposide caused an induction of apoptosis in thymocytes, as determined by the increase in cells exhibiting high blue fluorescence compared to control cells (compare regions 1 in Fig. 1a, b and c). Etoposide (1–25  $\mu\text{M}$ ) caused a time- (results not shown) and concentration-dependent increase in apoptotic cells without any marked increase in cytotoxicity, as assessed by the number of cells including propidium iodide, within the 4 hr incubation period (Table 1). Support for this conclusion was obtained by the concentration-dependent increase in DNA fragmentation caused by etoposide (Table 1). The proportion of cells undergoing apoptosis, as determined by flow cytometry, correlated with the amount of DNA fragmentation ( $r = 0.98$ ) (Table 1). Dexamethasone, a glucocorticoid, well known to induce apoptosis in thymocytes [5], was included as a positive control (Table 1). Further support for the induction of apoptosis was obtained from the results of the agarose gel electrophoresis, when etoposide

caused a concentration-dependent induction of internucleosomal cleavage of DNA (Fig. 2).

### Inhibition of etoposide-induced apoptosis

The induction of apoptosis by etoposide was inhibited by cycloheximide and actinomycin D, as assessed by flow cytometry (Table 2) and agarose gel electrophoresis (Fig. 3). Zinc inhibited etoposide-induced fragmentation as assessed by agarose gel electrophoresis (Fig. 3) and DNA fragmentation (Table 2) but not when assessed by flow cytometry (Fig. 1d and Table 2). In some early experiments, zinc caused some inhibition of the high blue fluorescent cells but no inhibition was observed in any of our recent studies. The reason for this variability is not known. As we have recently shown that zinc prevented dexamethasone-induced internucleosomal cleavage, but did not prevent certain key ultrastructural changes, we investigated the effects of zinc on etoposide-induced apoptosis.

### Characterization of Percoll-fractionated cells following exposure to etoposide alone or in the presence of zinc

The higher density of apoptotic compared with normal thymocytes has been used as the basis for their separation and purification, using discontinuous Percoll gradients [22]. Thymocytes were incubated for 4 hr with etoposide (10  $\mu\text{M}$ ) either alone or in the presence of zinc (1 mM) and separated on Percoll gradients into four discrete fractions (F1–F4), which were examined by flow cytometry, gel electrophoresis and electron microscopy. Cells in F2 and F4 have been best characterized and shown to correspond to normal and apoptotic cells, respectively [22]. Cells in F1 also have a normal morphology and contain a large number of proliferatively competent cells [22], whilst those in F3 contain preapoptotic thymocytes at an early stage of apoptosis [25]. Control thymocytes yielded predominantly only two fractions (F1 and F2). Agarose gel electrophoresis of the cells from the different Percoll fractions obtained following exposure to etoposide showed little or no DNA laddering in these supposedly normal cells (Fig. 4a

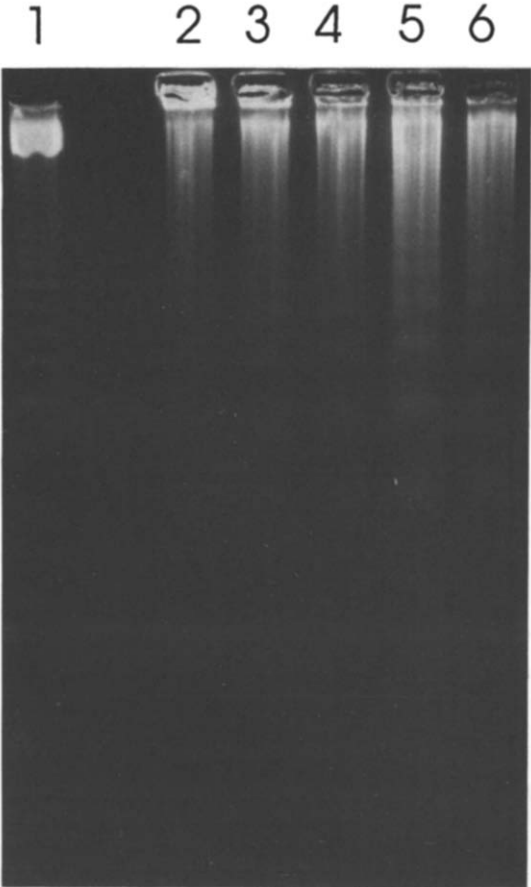


Fig. 2. Induction of internucleosomal DNA cleavage by etoposide. Thymocytes were incubated for 4 h either alone (lane 2, control) or in the presence of etoposide (1, 5 or 25  $\mu$ M, lanes 3–5, respectively) or dexamethasone (0.1  $\mu$ M, lane 6). The cells were then examined by agarose gel electrophoresis [23] for evidence of DNA laddering. Lane 1 contains markers of 123 bp or multiples thereof.

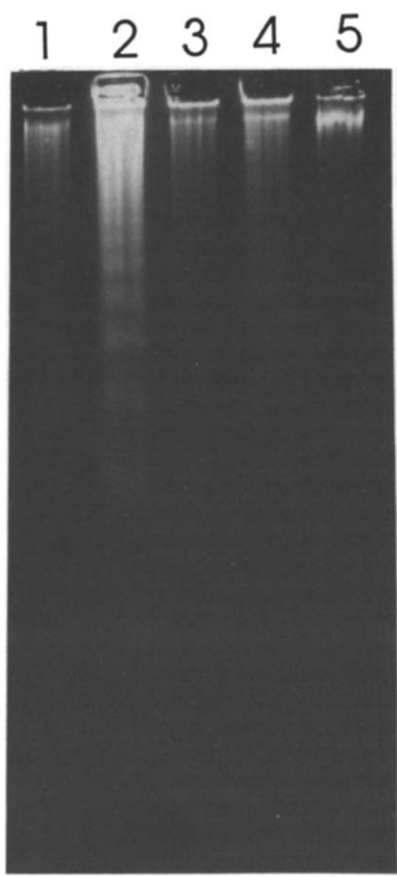


Fig. 3. Inhibition of etoposide-induced DNA laddering by cycloheximide, actinomycin D and zinc. Thymocytes were incubated for 4 hr either alone (lane 1) or with etoposide (10  $\mu$ M) (lane 2) in the presence of cycloheximide (10  $\mu$ M) (lane 3), actinomycin D (1  $\mu$ M) (lane 4) or zinc acetate dihydrate (1 mM) (lane 5). The cells were examined for DNA laddering by agarose gel electrophoresis [23].

Table 2. Abrogation of etoposide induced apoptosis by various inhibitors

	Apoptotic cells (%)	DNA fragmentation (%)
Control	7.5 $\pm$ 0.3	5.7 $\pm$ 1.7
Etoposide	27.7 $\pm$ 0.7	32.3 $\pm$ 6.4
+ Cycloheximide (10 $\mu$ M)	9.1 $\pm$ 0.6	11.3 $\pm$ 2.4
+ Actinomycin D (1 $\mu$ M)	11.1 $\pm$ 0.7	8.6 $\pm$ 2.4
+ Zinc (1000 $\mu$ M)	26.3 $\pm$ 1.5	3.3 $\pm$ 1.4

Thymocytes were incubated for 4 hr with etoposide (10  $\mu$ M) either alone or in the presence of various inhibitors. The % apoptotic cells and DNA fragmentation were determined as described in the legend to Table 1. The results represent the mean  $\pm$  SEM (N  $\geq$  3).

and b), whereas extensive laddering was observed in the purported apoptotic cells in F4 as well as in the cells from F3 (Fig. 4c and d). No DNA laddering was observed in any of the four fractions obtained when etoposide was incubated in the presence of zinc (Fig. 4e–h).

*Flow cytometric analysis of Percoll-fractionated cells*

Cells in F1 and F2 in the presence (Fig. 4e and f) or absence of zinc (Fig. 4a and b), exhibited high forward scatter (indicative of larger size) and low blue fluorescence typical of normal cells. With etoposide alone, cells from F3 (Fig. 4c) appeared heterogenous containing both apparently normal cells, which exhibited low blue fluorescence and also smaller cells with high blue fluorescence. Further incubation of cells, exhibiting low blue fluorescence, purified by fluorescence-activated cell sorting, resulted in the formation of smaller cells with high blue fluorescence (results not shown). Cells in F4 (Fig. 4d), following exposure to etoposide alone, were predominantly of a smaller size (lower forward

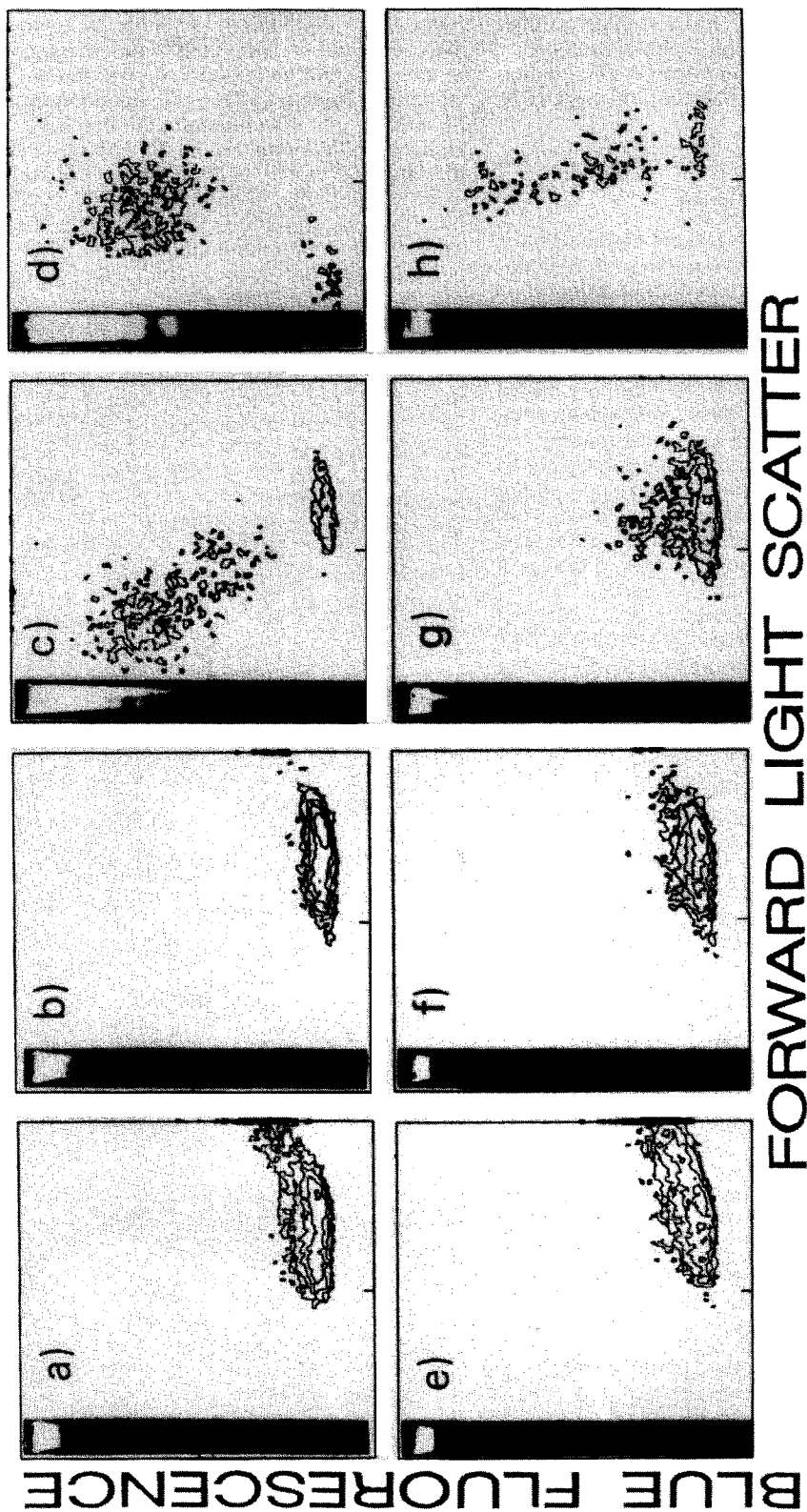


Fig. 4. Flow cytometric and agarose gel electrophoretic analysis of cells fractionated from Percoll. Thymocytes were incubated for 4 hr with etoposide (10  $\mu$ M) either alone (a–d) or in the presence of zinc (1 mM) (e–h). The cells were then separated on Percoll and DNA laddering assessed by agarose gel electrophoresis or incubated with Hoechst 33342 for 10 min as described in Materials and Methods and propidium iodide added before examination by flow cytometry. Normal and apoptotic cells exhibit low and high blue fluorescence, respectively. Forward light scatter gives an indication of cell size. Fractions F1 (a, e), F2 (b, f), F3 (c, g), and F4 (d, h) represent the four fractions of increasing density obtained from the Percoll separation.

light scatter) and exhibited high blue fluorescence with Hoechst 33342. Treatment with etoposide in the presence of zinc resulted in cells in F3, which were somewhat smaller (lower forward light scatter) and mainly exhibited low blue fluorescence (Fig. 4g), whilst the cells in F4 demonstrated a continuum of fluorescence intensities from low to high (Fig. 4h).

#### *Morphology of Percoll-fractionated cells*

The ultrastructure of cells treated with etoposide either alone, or in the presence of zinc, and separated into F1 and F2 resembled that of normal thymocytes. Following incubation with etoposide alone, cells in F4 contained typical apoptotic thymocytes which exhibited a regular, shrunken appearance with a condensed cytoplasm (Fig. 5a). Most organelles retained their normal appearance, although minimal swelling was observed in a few mitochondria and there was considerable dilation of many cisternae of the smooth endoplasmic reticulum. Fusion of the resulting vesicles with the cell membrane resulted in the characteristic cytoplasmic "bubbling" of apoptotic thymocytes (Fig. 5a). The nuclei were also shrunken and, although the euchromatin retained its normal appearance, the heterochromatin was condensed and usually coalesced against one pole of the nuclear membrane. The nucleus was often closely associated with the periphery of the cell and this usually resulted in the loss of a clear distinction between nuclear and cell membranes. This apparent coalescence of the two membranes could not be attributed to any obliquity of the sections. Most nuclei showed signs of nucleolar disintegration with several discrete clumps of particulate dense fibrillar components, which indicated dispersion of the transcriptional component from the fibrillar centre. Nuclear pores were rarely evident but the nuclear membrane of many of these cells was disrupted to such an extent that demarcation between the region of the particulate dense fibrillar components and that of the cytoplasmic organelles was indistinct.

Cells incubated with etoposide in the presence of zinc also yielded an F4 fraction of shrunken thymocytes with regular profiles. These thymocytes exhibited rather less dilation of the smooth endoplasmic reticulum and little cytoplasmic "bubbling". The nuclear membrane was usually intact, but convoluted, and the euchromatin retained its normal density. The euchromatin often included one or more clusters of intensely stained nucleolar remnants but these remnants were usually stained less intensely than those present in cells incubated with etoposide alone. The heterochromatin was arranged in several sharply defined clumps, which were contiguous with the nuclear membrane (Fig. 5b). The intervening regions of the nuclear membrane were devoid of any trace of heterochromatin but they did retain nuclear pores. A clump of condensed chromatin, similar to those associated with the nuclear membrane was present in the centre of many of these nuclei. Continuity was often observed between this central region and one or more of the peripheral clumps of condensed chromatin.

#### DISCUSSION

Etoposide caused a concentration-dependent induction of apoptosis in immature rat thymocytes. This conclusion was based on a number of criteria including increased DNA fragmentation and laddering (Table 1 and Fig. 2), increased formation of smaller cells with high blue fluorescence due to Hoechst 33342 (Table 1 and Fig. 1) and increased formation of small high density cells with the morphological characteristics of apoptosis obtained following isopycnic centrifugation (Fig. 5a). The inhibition of etoposide-induced apoptosis by cycloheximide and actinomycin D (Table 2) suggested that the induction of apoptosis was dependent upon new RNA and protein expression, as reported for glucocorticoid-induction of apoptosis in thymocytes [25, 26]. These results are in good agreement with those of Walker *et al.* [19], although our studies indicate less extensive inhibition of DNA laddering by actinomycin D (Fig. 3). The requirement for new RNA and protein synthesis in the induction of apoptosis appears to be dependent on the particular cellular system studied [3, 27].

A number of studies in thymocytes and other cellular systems have recognised zinc as an inhibitor of apoptosis, most probably due to its inhibition of the endonuclease [28, 29]. In agreement with these studies, zinc had a profound effect on etoposide-induced DNA fragmentation (Table 2) and DNA laddering (Fig. 3). However, zinc did not inhibit etoposide-induced apoptosis as assessed by flow cytometry (Table 2) in agreement with recent observations of the inability of zinc to inhibit dexamethasone-induced apoptosis [20, 30]. The apparent discrepancy of zinc inhibiting apoptosis as assessed by inhibition of DNA laddering (Fig. 3) but not as assessed by flow cytometry (Table 2) may be explained by its ability to inhibit the endonuclease [28, 29] whilst not affecting the increase in permeability of the apoptotic thymocytes responsible for the more rapid uptake of Hoechst 33342 and the higher blue fluorescence of these cells [31]. Of the four discrete fractions obtained following Percoll separation of cells treated with etoposide in the presence of zinc, F4 was of particular significance. These cells were smaller and denser than normal, exhibited high blue fluorescence with Hoechst 33342 but showed little or no DNA laddering or DNA fragmentation (Fig. 4h). In these cells, the heterochromatin was condensed and arranged in sharply defined clumps, abutting the nuclear membrane (Fig. 5b). These ultrastructural changes were clearly distinct from those observed with etoposide alone and resemble those described as the earliest ultrastructural features of apoptosis [32, 33]. These changes were accompanied by nucleolar disintegration, which appeared to involve dissociation of the dense fibrillar component from the fibrillar centre and its digestion into groups of dense particles. The formation of such particles has been attributed to cleavage of transcriptionally active ribosomal genes (rDNA) within the dense fibrillar components [6]. Other morphological features of apoptosis included cell shrinkage and the dilation of cisternae of the smooth endoplasmic reticulum, in the absence of

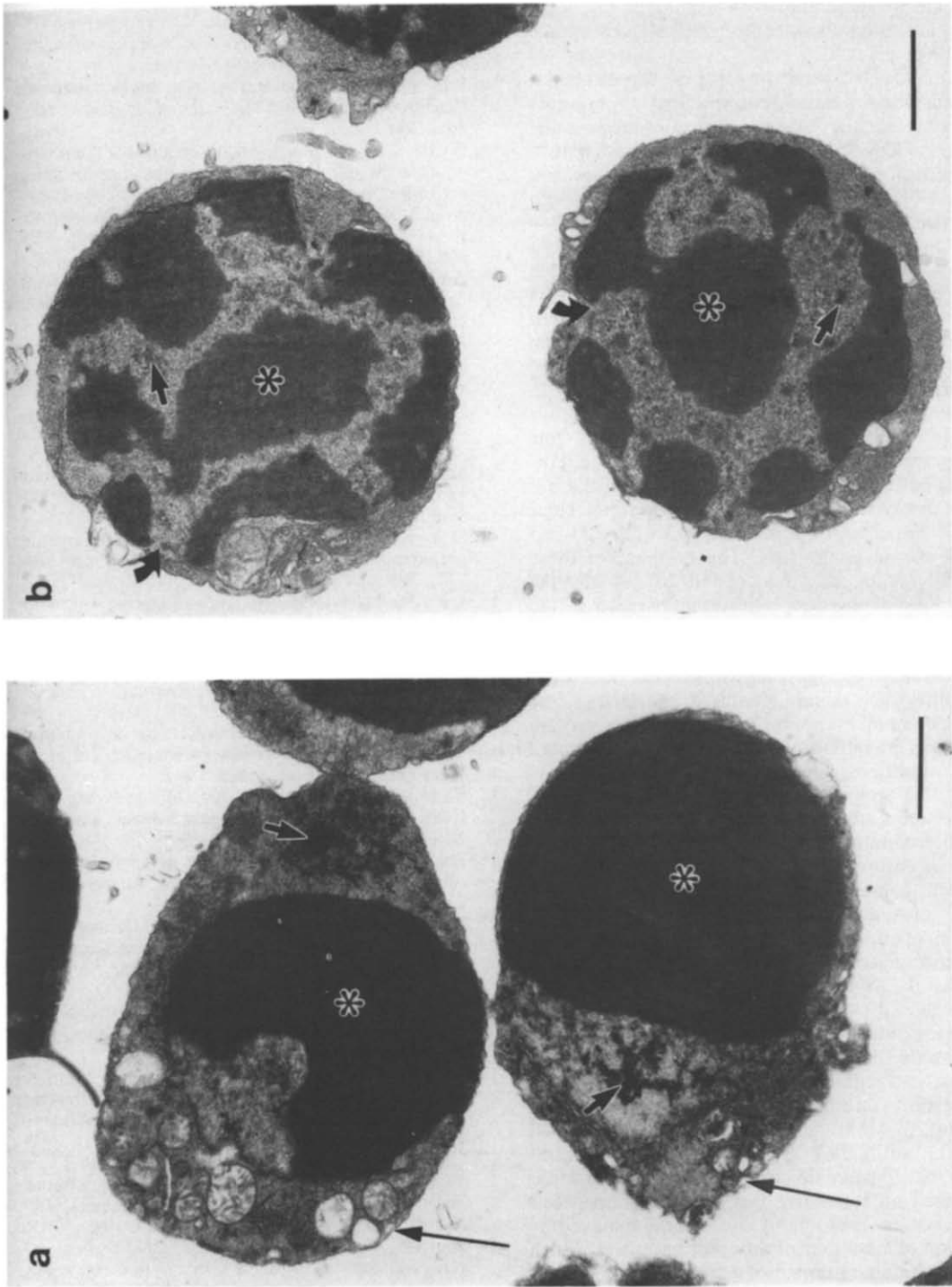


Fig. 5. (a) Cells concentrated in the F4 Percoll fraction following incubation of thymocytes with etoposide. The cytoplasm contained dilated cisternae of smooth endoplasmic reticulum, which fused with the cell membrane (arrows). The heterochromatin (\*) was condensed and coalesced against one pole of the nuclear membrane. Discrete clumps of dense fibrillar components (arrowheads) were evident but the nuclear membrane was discontinuous. Bar = 1 μm. (b) Cells in the F4 fraction from thymocytes incubated with etoposide in the presence of zinc exhibited rather less dilation of the smooth endoplasmic reticulum. The nuclear membrane was intact but convoluted. The euchromatin included clusters of nucleolar remnants (arrowheads). A sharply defined clump of moderately condensed heterochromatin (\*) was present in the centre of many of the nuclei. Similar clumps were contiguous with the nuclear membrane but the intervening regions of the nuclear membrane, which retained nuclear pores (curved arrows), were devoid of any trace of heterochromatin. Bar = 1 μm.

swelling in any other cytoplasmic organelles. These results demonstrated that, in the presence of zinc, etoposide induced many key features of apoptosis without any evidence of DNA laddering. We have recently observed similar effects on dexamethasone-induced apoptosis in the presence of zinc [20]. These results are in agreement with a number of recent studies, including oligodendrocytes [34], embryonic C3H/10T $\frac{1}{2}$  cells [35] and several instances of programmed cell death in insects [36], reporting that cell death with the classical morphology of apoptosis may occur in the absence of internucleosomal cleavage of DNA. Our results also suggest that in the induction of apoptosis, critical changes occur in nuclear DNA prior to endonuclease cleavage into nucleosomal fragments. In HL-60 cells exposed to etoposide, zinc inhibits DNA fragmentation but not the initial number of DNA strand breaks [37]. Such strand breaks, at particularly susceptible sites in DNA, may result in the morphological pattern observed in our studies (Fig. 5b). Zinc has been shown to modulate topoisomerase II induced apoptosis in HL-60 cells without any alteration in topoisomerase-mediated primary DNA strand breaks [38]. Recently, we have shown that whilst zinc completely inhibited dexamethasone-induced internucleosomal fragmentation of thymocytes, it did not prevent the cleavage of DNA into large molecular weight fragments of approximately 30–50, 200–245 and 700 kbp in length [39]. The presence of these large fragments may be related to the distinct morphology of the apoptotic cells observed in the presence of etoposide and zinc (Fig. 5b). Whilst our results are consistent with a role for zinc in inhibiting the endonuclease [26], they do not exclude other possibilities such as zinc binding to the DNA. Zinc may also modify apoptosis by activating protein kinase C or by inhibiting phosphorylases associated with inositol phosphate metabolism [40].

Our data support the hypothesis that zinc has arrested etoposide-induced apoptosis at an early stage, before internucleosomal DNA fragmentation [20]. Key early steps in apoptosis, which result in chromatin condensation, reduction in cell size and dilation of the endoplasmic reticulum, may thus occur independently of endonuclease cleavage of DNA into nucleosomal fragments. Internucleosomal cleavage of DNA resulting in "DNA ladders" has been regarded by many investigators as a *sine qua non* for the induction of apoptosis [3], but our results demonstrate that it may be a late event rather than a critical early step in this process. One such step may involve interference with topoisomerase II function [29]. Many agents including glucocorticoids, anti-CD3 antibodies,  $\gamma$ -irradiation, 2,3,7,8-tetrachlorodibenzo-*p*-dioxin, tributyltin oxide and topoisomerase I and II reactive drugs can induce apoptosis in thymocytes. Presumably this can be achieved by activation of a number of different pathways, which result in a smaller number of common intermediates leading to apoptosis.

**Acknowledgements**—We thank M. Lee and S. Preston for technical assistance and Mrs Gillian Zdaniecki for preparation of the manuscript.

## REFERENCES

1. Wyllie AH, Kerr JFR and Currie AR, Cell death: the significance of apoptosis. *Int Rev Cytol* **68**: 251–306, 1980.
2. Arends MJ and Wyllie AH, Apoptosis: mechanisms and roles in pathology. *Int Rev Exp Pathol* **32**: 223–254, 1991.
3. Cohen JJ, Duke RC, Fadok VA and Sellins KS, Apoptosis and programmed cell death in immunity. *Annu Rev Immunol* **10**: 267–293, 1992.
4. Ellis RE, Yuan J and Horvitz HR, Mechanisms and functions of cell death. *Annu Rev Cell Biol* **7**: 663–698, 1991.
5. Wyllie AH, Glucocorticoid-induced thymocyte apoptosis is associated with endogenous endonuclease activation. *Nature* **284**: 555–556, 1980.
6. Arends MJ, Morris RG and Wyllie AH, Apoptosis: the role of the endonuclease. *Am J Pathol* **136**: 593–608, 1990.
7. Aw TY, Nicotera P, Manzo L and Orrenius S, Tributyltin stimulates apoptosis in rat thymocytes. *Arch Biochem Biophys* **283**: 46–50, 1990.
8. Raffray M and Cohen GM, Bis(tri-*n*-butyltin)oxide induces programmed cell death (apoptosis) in immature rat thymocytes. *Arch Toxicol* **65**: 135–139, 1991.
9. Dive C and Hickman JA, Drug-target interactions: only the first step in the commitment to a programmed cell death. *Br J Cancer* **64**: 192–196, 1991.
10. Sen S and D'Incalci M, Apoptosis: biochemical events and relevance to cancer chemotherapy. *FEBS Lett* **307**: 122–127, 1992.
11. D'Arpa P and Liu LF, Topoisomerase-targeting antitumour drugs. *Biochim Biophys Acta* **989**: 163–177, 1989.
12. Liu LF, DNA topoisomerase poisons as antitumor drugs. *Annu Rev Biochem* **58**: 351–375, 1989.
13. Glisson BS and Ross WE, DNA topoisomerase II: a primer on the enzyme and its unique role as a multidrug target in cancer chemotherapy. *Pharmacol Ther* **32**: 89–106, 1987.
14. Zwelling LA, Topoisomerase II as a target of antileukemia drugs: a review of controversial areas. *Hum Pathol* **3**: 101–112, 1989.
15. Bertrand R, Kerrigan D, Sarang M and Pommier Y, Cell death induced by topoisomerase inhibitors. *Biochem Pharmacol* **42**: 77–85, 1991.
16. Zhang H, D'Arpa P and Liu LF, A model for tumor cell killing by topoisomerase poisons. *Cancer Cells* **2**: 23–27, 1990.
17. Berger NA, Chatterjee S, Schmotzer JA and Helms SR, Etoposide (VP-16-213)-induced gene alterations: potential contribution to cell death. *Proc Natl Acad Sci USA* **88**: 8740–8743, 1991.
18. Chow K-C, King CK and Ross WE, Abrogation of etoposide-mediated cytotoxicity by cycloheximide. *Biochem Pharmacol* **37**: 1117–1122, 1988.
19. Walker PR, Smith C, Youdale T, Leblanc J, Whitfield JF and Sikorska M, Topoisomerase II-reactive chemotherapeutic drugs induce apoptosis in thymocytes. *Cancer Res* **51**: 1078–1085, 1991.
20. Cohen GM, Sun X-M, Snowden RT, Dinsdale D and Skilleter DN, Key morphological features of apoptosis may occur in the absence of internucleosomal DNA fragmentation. *Biochem J* **286**: 331–334, 1992.
21. Sun X-M, Snowden RT, Skilleter DN, Dinsdale D, Ormerod MG and Cohen GM, A flow cytometric method for the separation and quantitation of normal and apoptotic thymocytes. *Anal Biochem* **204**: 351–356, 1992.
22. Wyllie AH and Morris RG, Hormone-induced cell death: purification and properties of thymocytes undergoing apoptosis after glucocorticoid treatment. *Am J Pathol* **109**: 78–87, 1982.



23. Sorenson CM, Barry MA and Eastman A, Analysis of events associated with cell cycle arrest at G2 phase and cell death induced by cisplatin. *J Natl Cancer Inst* **82**: 749–755, 1990.
24. Burton K, A study of the conditions and mechanisms of the diphenylamine reaction for the colorimetric estimation of deoxyribonucleic acid. *Biochem J* **62**: 315–323, 1956.
25. Cohen GM, Sun X-M, Snowden RT, Ormerod MG and Dinsdale D, Identification of a transitional preapoptotic population of thymocytes. *J Immunol* **151**: 566–574, 1993.
26. Wyllie AH, Morris RG, Smith AL and Dunlop D, Chromatin cleavage in apoptosis: association with condensed chromatin morphology and dependence on macromolecular synthesis. *J Pathol* **142**: 67–77, 1984.
27. Martin SJ, Lennon SV, Bonham AM and Cotter TG, Induction of apoptosis (programmed cell death) in human leukemic HL-60 cells by inhibition of RNA or protein synthesis. *J Immunol* **145**: 1859–1867, 1990.
28. Cohen JJ and Duke RC, Glucocorticoid activation of a calcium-dependent endonuclease in thymocyte nuclei leads to cell death. *J Immunol* **132**: 38–42, 1984.
29. Giannakis C, Forbes IJ and Zalewski PD,  $\text{Ca}^{2+}/\text{Mg}^{2+}$ -dependent nuclease: tissue distribution, relationship to inter-nucleosomal DNA fragmentation and inhibition by  $\text{Zn}^{2+}$ . *Biochem Biophys Res Commun* **181**: 915–920, 1991.
30. Barbieri D, Troiano L, Grassilli E, Agnesini C, Cristofalo EA, Monti D, Capri M, Cossarizza A and Franceschi C, Inhibition of apoptosis by zinc: a reappraisal. *Biochem Biophys Res Commun* **187**: 1256–1261, 1992.
31. Ormerod MG, Sun X-M, Snowden RT, Davies R, Fearnhead H and Cohen GM, Increased membrane permeability of apoptotic thymocytes: a flow cytometric study. *Cytometry* **14**: 595–602, 1993.
32. Kerr JFR, Searle J, Harmon BF and Bishop CJ, Apoptosis. In: *Perspectives on Mammalian Cell Death* (Ed. Potten CS), pp. 93–128. Oxford University Press, New York, 1987.
33. Walker NI, Harmon BV, Gobé GC and Kerr JFR, Patterns of cell death. *Methods Achiev Exp Pathol* **13**: 18–54, 1988.
34. Barres BA, Hart K, Coles HSR, Burne JF, Voyvodic JT, Richardson WD and Raff MC, Cell death and control of cell survival in the oligodendrocyte lineage. *Cell* **70**: 31–46, 1992.
35. Tomei LD, Shapiro JP and Cope FO, Apoptosis in C3H/10T $\frac{1}{2}$  mouse embryonic cells: Evidence for internucleosomal DNA modification in the absence of double-strand cleavage. *Proc Natl Acad Sci USA* **90**: 853–857, 1993.
36. Lockshin RA and Zakeri Z, Programmed cell death and apoptosis. In: *Apoptosis: The Molecular Basis of Cell Death* (Eds. Tomei LD and Cope FO), pp. 47–60. Cold Spring Harbor Laboratory Press, 1991.
37. Shimizu T, Kubota M, Tanizawa A, Sano H, Kasai Y, Hashimoto H, Akiyama Y and Mikawa H, Inhibition of both etoposide-induced DNA fragmentation and activation of poly (ADP-ribose) synthesis by zinc ion. *Biochem Biophys Res Commun* **169**: 1172–1177, 1990.
38. Bertrand R, Solary E, Jenkins J and Pommier Y, Apoptosis and its modulation in human promyelocytic HL-60 cells treated with DNA topoisomerase I and II inhibitors. *Exp Cell Res* **207**: 388–397, 1993.
39. Brown DG, Sun X-M and Cohen GM, Dexamethasone-induced apoptosis involves cleavage of DNA to large fragments prior to internucleosomal fragmentation. *J Biol Chem* **268**: 3037–3039, 1993.
40. Waring P, Kos FJ and Müllbacher A, Apoptosis or programmed cell death. *Med Res Rev* **11**: 219–236, 1991.